The influence of nanodiamond on the oxygenation states and micro rheological properties of human red blood cells *in vitro*

Yu-Chung Lin
Lin-Wei Tsai
Elena Perevedentseva
Hsin-Hou Chang
Ching-Hui Lin
Der-Shan Sun
Andrei E. Lugovtsov
Alexander Priezzhev
Jani Mona
Chia-Liang Cheng

The influence of nanodiamond on the oxygenation states and micro rheological properties of human red blood cells *in vitro*

Yu-Chung Lin,[a] Lin-Wei Tsai,[a] Elena Perevedentseva,[a,b] Hsin-Hou Chang,[c] Ching-Hui Lin,[c] Der-Shan Sun,[c] Andrei E. Lugovtsov,[d] Alexander Priezzhev,[d] Jani Mona,[a] and Chia-Liang Cheng[a]
[a]National Dong Hwa University, Department of Physics, Hualien 97401, Taiwan
[b]P. N. Lebedev Physics Institute, Russian Academy of Science, 119991 Moscow, Russia
[c]Tzu-Chi University, Department of Molecular Biology and Human Genetics, Hualien, Taiwan
[d]M.V. Lomonosov Moscow State University, Physics Department and International Laser Center, 119991 Moscow, Russia

Abstract. Nanodiamond has been proven to be biocompatible and proposed for various biomedical applications. Recently, nanometer-sized diamonds have been demonstrated as an effective Raman/fluorescence probe for bio-labeling, as well as, for drug delivery. Bio-labeling/drug delivery can be extended to the human blood system, provided one understands the interaction between nanodiamonds and the blood system. Here, the interaction of nanodiamonds (5 and 100 nm) with human red blood cells (RBC) *in vitro* is discussed. Measurements have been facilitated using Raman spectroscopy, laser scanning fluorescence spectroscopy, and laser diffractometry (ektacytometry). Data on cell viability and hemolytic analysis are also presented. Results indicate that the nanodiamonds in the studied condition do not cause hemolysis, and the cell viability is not affected. Importantly, the oxygenation/deoxygenation process was not found to be altered when nanodiamonds interacted with the RBC. However, the nanodiamond can affect some RBC properties such as deformability and aggregation in a concentration dependent manner. These results suggest that the nanodiamond can be used as an effective bio-labeling and drug delivery tool in ambient conditions, without complicating the blood's physiological conditions. However, controlling the blood properties including deformability of RBCs and rheological properties of blood is necessary during treatment. © *2012 Society of Photo-Optical Instrumentation Engineers (SPIE).* [DOI: 10.1117/1.JBO.17.10.101512]

Keywords: red blood cell; hemoglobin; nanodiamond; bio-labeling; Raman spectroscopy; deformability index.

Paper 12084SS received Feb. 7, 2012; revised manuscript received Apr. 18, 2012; accepted for publication Apr. 30, 2012; published online Jun. 14, 2012.

1 Introduction

Recently, nanodiamond (ND) has been proposed to be an effective nano-bio-probe utilizing its unique Raman[1,2] and fluorescence[3] signals. Surface functionalized ND finds substantial progress for different applications such as conjugations of drugs for effective drug delivery, nanosurgery, and prosthetic devices for retinal implants.[4–6] The NDs have been proven to be an ideal biocompatible platform, while Raman and fluorescence signals serve as markers in various biomedical applications.[1–6]

Raman spectroscopy is also suitable for investigating blood protein such as hemoglobin (Hb) and red blood cells (RBC).[7–9] Raman spectrum signal observed for Hb is strong but relatively complex; however, there are certain trivial footprints from Hb states, which can be used to draw important conclusions for studying the RBC.[8] Particularly one can study the oxygenation and spin state dynamics of the heme (the active center of Hb) due to a selective enhancement of the Raman active vibrations in different oxygenation states. Owing to variations in the oxygenation states of Hb, the spectrum exhibits dramatic changes in the spin state regions (1500 to 1650 cm^{-1}) and the methane C-H deformation region (1200 to 1250 cm^{-1}) followed by $T \leftrightarrow R$ (tense-relaxed transition).[7] These dramatic changes in the spin state regions and associated structural changes

(at $T \leftrightarrow R$) of the heme and Hb globule can be studied *in situ* using Raman spectroscopy.[8] Additionally, heme orientation is an important factor in RBCs' functions. Raman spectroscopy has already been demonstrated as an imperative tool to study the heme ordering in functional RBC and the laser-induced effect[9,10] to monitor changes in the oxygenation state of human RBCs while they were placed under mechanical stress.[11]

For the successful development of ND for bio-labeling and for drug delivery, the most critical feature for considering them for biomedical applications is their interaction mechanism with the RBC and ultimately with the heme. Even though previous studies have confirmed low *in vitro* cytotoxicity offered by the NDs, for the *in vivo* studies, studying ND interactions with living organisms as well as with organs and tissues, especially with blood, like integrative tissue, is necessary.[12,13]

Among the constituents of blood, RBCs are major oxygen carriers for the circulating system, and Hb is the major protein component in RBC, which is responsible for the reversible oxygen carrying and storage. The RBCs do not reveal any phagocytosis and endocytosis, so other mechanisms including diffusion, transmembrane channels, adhesive interaction via electrostatic, Van der Waals and hydration forces, or steric interactions may be involved.[14] Reports revealed that certain fine nanoparticles with size less than 200 nm can enter easily

Address all correspondence to: Chia-Liang Cheng, National Dong Hwa University, Department of Physics, Hualien 97401, Taiwan. Tel: +88638633696; Fax: +88638633690; E-mail: clcheng@mail.ndhu.edu.tw

inside the RBC, and the larger ones are associated with the membrane.[14,15] Different effects of nanoparticles on blood/blood components, and biocompatibility have been discussed using mesoporous silica,[16] gold nanoparticles,[17] magnetite Fe_3O_4 nanoparticles,[18] and TiO_2.[19] Mostly, hemolytic properties are used as one of the common tests for understanding nanoparticle interactions. Few studies[12] of ultrafine detonation nanodiamond with whole blood show some harmful effects on blood's biochemical characteristics, but serious blood cell destruction was not observed. On the other hand, the attachment of polystyrene nanoparticles (100 to 1100 nm) with modified surfaces to RBC increases the circulation lifetime of these drug delivering particles.[20,21] However for the development of the *in vivo* bio applications of ND, serious study on ND interactions with blood (whole blood as well as blood components) is vital.

In the present work, we have studied the interaction of ND (5 and 100 nm) with human RBCs. Confocal microscopy has been used to observe ND attaching on the RBC membrane, penetration inside (only 5 nm ND) the RBC, and interaction of nanodiamond with the membrane. Raman spectroscopy and UV-visible absorption are used to characterize the effect of ND on the oxygenation and deoxygenation processes of RBC. Further, interaction of ND with RBC membrane is presented with the help of RBC deformability analysis. In addition, the ND hemolytic ability and cytotoxicity properties are also discussed.

2 Experimental Procedures

All experiments using human subjects were coherent to the national regulation of Human Subject Research (Taiwan) and the Declaration of Helsinki. To achieve the purpose, we had formally obtained informed written and signed consent for all volunteers; the PI, as well as the students who performed the experiments had taken lectures concerning ethical issues.

2.1 Nanodiamond Carboxylation

Synthetic diamond powders with an average size of 5 nm (Microdiamant AG Switzerland) and 100 nm (Kay Diamond, USA) were carboxylated/oxidized (referred to as cND) according to methods described elsewhere in detail to remove surface impurity or defects.[5,22] Fourier transform infrared (FTIR) Spectroscopy (Bomen MB 154, Canada) was used to analyze the cND's surface functional groups. FTIR spectra of these dried samples show the well-resolved line of C = O stretching of carbonyl group on the nanodiamond surface in the range of 1720 to 1780 cm^{-1} as seen from the previous reports.[22]

2.2 Red Blood Cells (RBC) Sample Preparation

Five milliliters of whole blood was drawn from each healthy volunteer and was transferred into EDTA-covered tubes. The RBCs were separated from the human blood using centrifugation with the speed 1500 rpm (250 g) for 5 min at 4°C. RBC mass was further separated from the supernatant plasma and then washed with standard phosphate buffer saline (PBS: NaCl 0.4 g; KCl 0.01 g, Na_2HPO_4 0.072 g, KH_2PO_4 0.021 g; H_2O 50 ml; pH 7.05). Concentrations of PBS to RBC were 2 : 1 at 4°C and pH was maintained at the value of 7.4. RBC + PBS mixture was centrifuged at the rate of 3400 rpm (1281 g) for 1 min. This process was repeated 3 to 5 times. Finally, the washed RBCs were diluted with PBS in the ratio of 5 μl : 1000 μl (RBC : PBS).

2.3 Microscopic Investigation of cND Interaction with RBC

The interaction of cND with RBC and cND's effect on oxygenation-deoxygenation process of RBC were studied with 5 and 100 nm cNDs. The cNDs were suspended in PBS in 10 mg/ml concentration. From this suspension, 5 μl of the cND + PBS suspension was mixed with 1500 μl of PBS and was added to 1005 μl RBC + PBS suspension. A final concentration of cND in the prepared cND + RBC + PBS sample used for the measurements was ~20 μg/ml.

Fluorescence and optical (bright field, BF) images of cND interaction with the RBCs were observed using scanning fluorescence confocal microscope (TCS-SP5, Leica, Germany). To observe the fluorescence signal from the 5 and 100 nm sized cND, the excitation wavelengths used were 488 nm and 543 nm, the corresponding signal detection was between 491 to 539 nm and 562 to 659 nm. The wavelengths were selected according to the fluorescence spectra observed for the cND.[23] Fluorescence with the overlapped peaks in the region 495 to 525 nm mostly attributed to H^4 (3N-V-N or 3NV-V-N) and H^3 (N-V-N) defect centers (in present case excited with 488 nm), and NV^- centers fluorescence band centered at 670 nm (excited with 543 nm) were used. It is to be mentioned that weak Hb fluorescence at these excitations was also observed (data not shown), so in the Raman spectra, we had performed baseline correction to remove the fluorescence background. Confocal scanning was also performed along the Z-axis to probe the localization of cND relative to the RBC (data not shown).

2.4 Raman Investigation of cND Interaction with RBC

The Raman spectrum was measured using a Raman spectrometer (T64000, Jobin Yvon, France) with 532 nm excitation wavelength. For the Raman measurements, RBCs were suspended in the buffer solution. The RBC to PBS ratio used was 5 μl : 1000 μl and for the comparison the samples of cND+ RBC + PBS were prepared as described above. The prepared RBC + PBS and the cND + RBC + PBS suspensions were placed in a Petri dish of diameter 5 cm; a Si substrate 2×2 cm^2 was kept at the bottom during the initial microscopic measurements to avoid the interference of the signals from the plastic Petri dish. The oxygenation–deoxygenation process at cND's interaction with RBC was monitored via the changes of RBC's Raman spectra, which were taken every 5 min. Oxygenation was achieved in ambient atmospheric pressure, and deoxygenation was performed with nitrogen gas (10 kg/cm^2) purged into the Petri dish.

2.5 RBC Deformability Analysis

To study the possible effect of nanodiamonds on blood rheology we checked the flexibility of RBC, which characterize the ability of these cells to deform under shear stress passing through thin vessels and capillaries. For this purpose we measured the deformability index of RBC, which is relative elongation in dependence on the shear stress in the flow. Measurements were performed with in-house built device laser aggregometer-deformometer of erythrocytes. The schematic layout and detailed description of the device was reported previously.[24,25]

In this investigation, 5 ml of whole blood was drawn from each volunteer. The blood was drawn before meal in the morning, and the measurements were performed within two hours after blood drawing. There were a total of eight volunteers. All blood samples were stabilized with anticoagulant (7% solution of EDTA) in concentration of 0.15 ml of EDTA solution per 5 ml of whole blood, which allowed for avoiding the blood clotting during the experiment. Because RBC deformability depends on Hb oxygenation[26] the blood samples were oxygenated by repeated exposure to ambient air prior to the measurement. The whole blood portions in amount of 1 ml were incubated about 1 h with suspensions of 5 and 100 nm cND. Two different concentrations of nanodiamonds suspension were investigated: 30 and 100 μg/ml. After incubation with cND, the whole blood samples were highly diluted in order to ensure the single scattering regime, which is a necessary condition in laser diffractometry measurements. In order to raise the viscosity of the cell suspending fluid and thus obtain higher shear stresses at fixed shear rates, 6.5 μl of each sample of RBC with nanodiamonds was diluted with 1 ml of highly viscous isotonic solution (pH 7.4) consisting of distilled water, NaCl and polyox—an isotonic solution of high molecular mass polyethylenoxide in concentration 0.5% yielding the viscosity of 13 centipoises. Samples of RBC suspension with cND and without cND (control) were investigated by means of diffractometry technique, also known as ektacytometry. The dependences of deformability index on shear stress were obtained for each sample.

2.6 Cell Viability Analysis

The cell viability of RBC interaction with cND was estimated using WST-1 Tetrazolium dyes (Roche, Germany, provided by the manufacturer). WST-1 test is based on the principle that the enzyme in viable cell cleaves the Tetrazolium salt WST-1 and produces a soluble colored formazan salt, which is measured spectrophotometrically. The conversion is performed only by viable cells, which are correlated with the cell number. WST-1 has already been used to analyze the viability of various cell types[27] and was shown to be metabolized in the case of RBCs.[28] For the cell viability analysis, RBCs were prepared as described earlier.[29] A standard curve that was plotted between WST-1 values with the cND-treated RBCs was obtained first, and finally the relative amount of viable cells was calculated accordingly. These samples were compared with RBCs dissolved in PBS (untreated groups). The absorbance of the resulting supernatant fluid of untreated groups without cND was normalized to 100%. The data were obtained from three independent experiments.

2.7 Hemolysis Analysis

Hemolysis analysis was carried out at room temperature (25°C) with some modifications using a protocol as described in earlier reports.[30] Whole blood samples were first mixed (1 : 1; v/v) with anticoagulant acid citrate dextrose (ACD) solution. In the next step, cNDs of sizes 5 and 100 nm were added to the citrated blood samples (100 μl) in concentrations of 5 μg/ml and 50 μg/ml and were incubated for 3 h. Solutions were centrifuged at 160 g (1000 rpm) and 25°C, for 10 min. After centrifugation, the hemolytic levels of the resulting supernatant fluid were determined by measuring the absorbance at 540 nm with Hitachi 3300H spectrophotometer (Hitachi, Japan). RBCs added to the PBS and RBC + PBS added with Triton X-100 (diluted in normal saline (PBS), final concentration 0.5% (v/v) to study the negative control) were used for comparisons. The absorbance measured after Triton X-100 treatment was normalized to 100%. The data were collected from three independent experiments.

2.8 Statistical Analysis

All the results were calculated using data from at least three independent experiments. The T-test was used to assess the statistical significance of differences in antimicrobial effects. A P value of less than 0.05 ($P < 0.05$) was considered significant.

3 Results and Discussion

Figure 1 shows the fluorescence and merging optical (bright field) images of RBC interactions with 5 and 100 nm sized cND. Nanodiamond's intrinsic fluorescence has been used to image the locations of the cND. In this fluorescence imaging, the excitation wavelength used was 488 nm, and the fluorescence data were collected in the range of 491 to 539 nm. From Fig. 1(I) we observe that the 100 nm cND are localized on the RBC surface, whereas 5 nm cND penetrate inside the RBCs. Figure 1(II) depicts the z-scans of RBCs interacting with 100 nm cND of an individual RBC. It can be seen from the images of Fig. 1 (Ia to Ic), and particularly from the z-scans [Fig. 1(II)], that the cND with the particle size 100 nm interacts predominantly with the RBC membrane. As we already know from the earlier reports, a RBC does not reveal phagocytosis and endocytosis; however some nanoparticles with size less than 200 nm may penetrate the cell membrane,[14,15] so other mechanisms of nanoparticles-cell interaction can be involved. Contrary to this in our study, we do not observe 100 nm cND penetrations into a RBC, however penetration with smaller size (5 nm) were observed [Fig. 1(I)]. In addition, we observed that 5 nm cNDs induce the RBC aggregation even in PBS suspension [Fig. 1(II)]. Therefore, two important questions arise: first, how does the nanodiamond affect the RBC membrane; and second, can nanodiamond penetrate into the RBC and interact directly and affect the Hb state and functions? The present work is focused on the first question, and the second question will be considered in the course of future studies.

Results of cell viability, i.e., the WST-1 test on RBC interaction with 5 and 100 nm cND at concentrations of 5 μg/ml and 50 μg/ml, are presented in Fig. 2. It is observed that RBC cells are viable for interaction with both the 5 nm and 100 nm cND. The nanodiamond hemolytic effect was estimated for 5 and 100 nm cND. Also, different concentrations, 5 μg/ml and 50 μg/ml of cND incubated with RBCs were used. It was further compared with the hemolysis effect for RBCs treated with 0.5% Triton X-100 and with PBS. The absorbance of the supernatant fluids of differently treated RBCs were measured and compared. Interestingly, it can be seen from Fig. 3 that the hemolytic effect of cND does not exceed 2% to 4% as compared with hemolysis created by Triton X-100, which is 100%. There were no differences within standard deviation between PBS- (control) and cND treated samples.

Previously, in-vitro studies on various nanoparticles demonstrated the nanoparticle-induced hemolysis,[31] depending on the particles size, surface properties and experimental conditions.[19,32] It is known that nanoparticles can induce hemolysis directly affecting the membrane, or via oxidative stress (for example, TiO_2).[19] The adsorption of blood plasma proteins
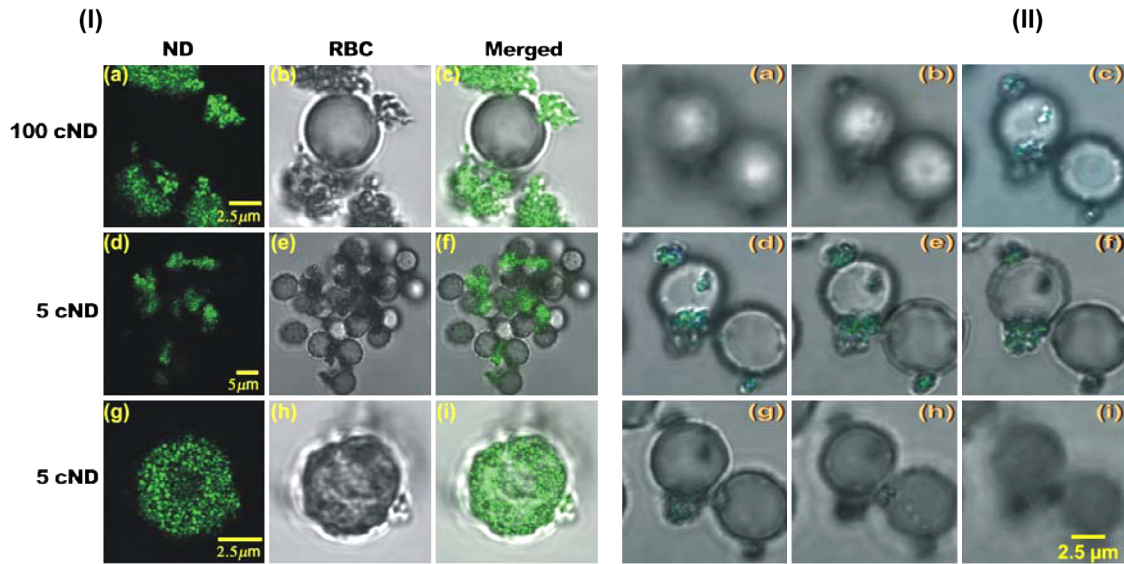
Fig. 1 Nanodiamond interaction with human red blood cells. (I) Fluorescence and bright field (BF) optical images of cND, RBCs and cND with sizes 100 and 5 nm at their interaction with RBCs. The cND fluorescence is excited with 488 nm and collected in the 491 to 539 nm range (shown in green). (II) A z-scan of 100 nm cND interacting with RBC. The images correspond to different positions along z-axis with 1 μm step. The cND fluorescence is excited with 543 nm and collected in range 562 to 659 nm (shown in green). The images indicate cNDs are attaching to the cell membrane of the RBC.
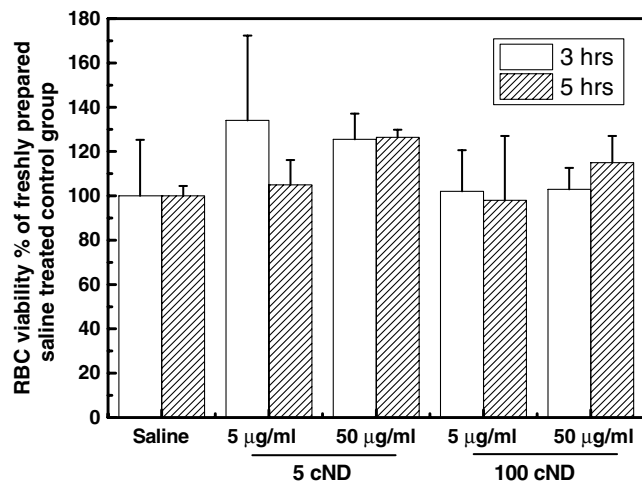
Fig. 2 RBC cell viability WST-1 test. Cell viability of RBC treated with normal saline (control) and cND's (size 5 and 100 nm cND) with concentrations 5 and 50 μg/ml in RBC suspension for 3 and 5 h. Data are reported as mean $\pm$ standard deviation (SD). Three independent experiments with two replicates ($n = 6$).
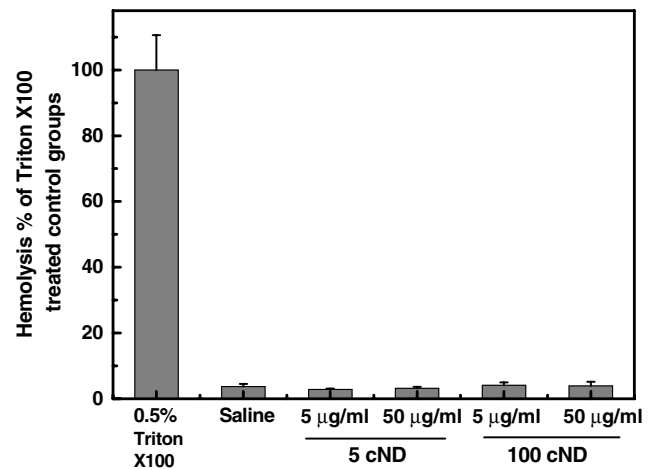

Fig. 3 Hemolytic effect of nanodiamond. After incubation with different concentration (5 and 50 μg/ml) of 5 and 100 nm cND for 3 h, the absorbance of the supernatant fluid of RBC was compared with 0.5% Triton ×100 and normal saline treated RBC. The absorbance of Triton ×100 groups was normalized to 100%. Data are reported as mean$\pm$ standard deviation (SD). Three independent experiments with two replicates ($n = 6$).

on NDs causes electrolyte and osmotic imbalance that results in cell destruction. Particularly, the RBC hemolysis during the interaction of whole blood with ultra-fine detonation nanodiamond was observed,[12] but was not estimated quantitatively. The present work shows quantitative information using 5 and 100 nm size cND. Figure 1 clearly demonstrates that cND is attached to RBC membrane, and a hemolysis test confirms the stability of the RBC membranes. Further, it is to be noted that in previous reports, the adsorption of blood plasma proteins on cND was analyzed, particularly, by varying pH, and it was shown that at pH near 7.4 the adsorbance of the main blood plasma proteins like albumin and immunoglobulin is low and varies for cND with various sizes and surface properties.[33,34]

Figure 4 displays the Raman spectra of oxygenated and deoxygenated RBCs interacting with 100 nm sized cND. Similar spectra were observed for 5 nm cNDs as well (spectra not shown). The spectra have been compared with RBC's spectra, which serve as reference. It is seen that the Raman spectrum does not reveal any structural transformations for RBCs (for Hb) due to the presence of cNDs. We have seen that cND can interact with RBC membrane and, correspondingly, interaction of cND with RBC membrane can change the membrane properties, and hence can change the conditions for gas transportation. This assumption is based on the fact that the penetration of oxygen (as well as CO_2 and some other small molecules) through RBC membrane depends on the membrane structure
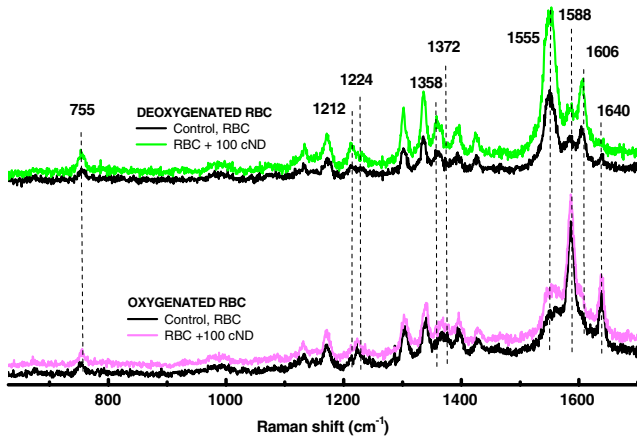
Fig. 4 Nanodiamond effects on the Raman spectra of RBC. Comparison of Raman spectra of oxygenated and deoxygenated RBC at interaction with 100 nm cND. The numbers mark the positions of major Raman peaks of RBC (in cm^{-1}).
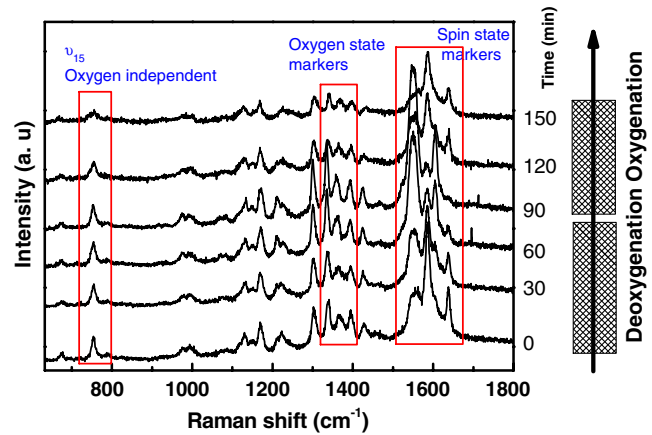

Fig. 5 Raman spectra of RBC at various oxygenation states. Raman spectra are measured *in-situ* in the oxygenation/deoxygenation process of a single RBC cell. RBC interacting with 100 nm cND are gradually deoxygenated and then re-oxygenated by purging N_2 through medium (PBS, pH = 7.4) of RBC suspension. The Raman spectra were obtained with 532 nm wavelength laser excitation, laser power ~1 mW, and a 60× water immersion objective. The nanodiamond concentration used was 20 μg/ml. The red boxes are indicating some affecting Raman peaks at various oxygenation degrees.

and state.[35] Particularly, when the membrane fluidity is altered (for example chemically, with forming cholesterol-enriched membrane),[36] the membrane rearrangement changes the oxygen transport. To analyze the effect of cND on this RBC function, we study the process of oxygenation/deoxygenation.

The oxygenation/deoxygenation analysis via Raman spectra (as seen in Fig. 4) can be explained as follows. The RBC Raman spectrum exhibits a number of peaks to characterize Hb at different states. The major differences in the spectra are attributed to changes in the spin state between the deoxygenated heme with Fe in high-spin ($S = 2$) state and the oxygenated heme with low-spin ($S = 1/2$) state Fe. Correspondingly, the spectrum is sensitive to the conformational changes in Hb molecules, i.e., Hb transition from relax (R) state (oxygenated Hb) to tense (T) state (deoxygenated Hb). The porphyrin perturbations in oxygenation-deoxygenation cycle are associated with the tense-relaxed ($T \leftrightarrow R$) state transition of hemoglobin (Hb) within a single red blood cell.[7] Deoxy-Hb is in the T-state with high-spin iron ($S = 2$; Fe^{2+}); the main bands for this state are observed at 1606 to 1610 (ν_{10}),1580 to 1582 (ν_{37}), 1544 to 1547 (ν_{11}), and 1210 to 1215 cm^{-1} ($\nu_5 + \nu_8$). Oxy-Hb is in R-state with low-spin Fe^{3+}($S = 1/2$); some intense bands are observed at 1636 to 1640 (ν_{10}), 1562 to 1565 (ν_2), 1245 to 1259 (ν_{13}), and 1224 to 1226 cm^{-1} ($\nu_5 + \nu_8$) and a few other bands for carboxylated Hb (Fe^{2+}) are exhibited.[8] The oxygenation degree of the samples can be monitored using the oxidation state marker bands (ν_4) in the ranges 1355 to 1380 cm^{-1} and 1500 to 1650 cm^{-1}, which are sensitive to the spin and coordination state of the heme. To estimate the Hb oxygenated state we chose the intense and accentuated bands, which serve as reference for characterizing the low spin state of heme. In the deoxygenated RBCs the principal band is used at 1604 to 1608 cm^{-1}, while for the oxygenated cells the bands used appear at 1638 to 1640 cm^{-1} and 1586 to 1588 cm^{-1}. The intensity of the band at 755 cm^{-1} (ν_{15}, a pyrrole breathing mode) does not depend on Hb oxygenation state and serves as a reference point for the estimation of the degree of oxygenation.[37,38] Figure 5 shows the Raman spectra of a single RBC with 100 nm ND at various oxygenation states during the process of deoxygenation (with N_2 purging), which is further followed by oxygenation (in air).

The cycle for deoxygenation followed by oxygenation is shown in Fig. 6. The oxygenation-deoxygenation cycle is characterized using the intensity ratio of peaks from 1640 cm^{-1} to 755 cm^{-1}. In the measurements shown in Fig. 6(a) and 6(b), 20 μg/ml of cND were used, and the curve for RBC sample is marked as solid squares, while the curve for RBC interacting with 100 nm [Fig. 6(a)] and 5 nm [Fig. 6(b)] cND is shown as red, solid circles. The intensity ratios are plotted as a function of oxygenation/deoxygenation time. It can be seen that the 100 nm cNDs does not greatly affect the deoxygenation dynamics of the RBC. However, some delay of the oxygenation is observed for the deoxygenated RBC with 100 nm cND, and the effect is more significant for 5 nm cND. Figure 6(c) shows that this effect of 100 nm cND on the RBC oxygenation/deoxygenation cycle is concentration dependent.

Analogous to Fig. 6, the oxygenation-deoxygenation cycle of RBC and RBC interacting with cND is characterized using the intensity ratio of peaks for oxygenated state at 1588 cm^{-1}, and for deoxygenated state at 1555 cm^{-1} (attributed as ν_{19} or ν_{37}).[37] The dependencies of the peak ratio [$PR = I_{1588}/(I_{1555} + I_{1588})$] on time, during deoxygenation followed by re-oxygenation, are presented in Fig. 7. Fittings were done using standard second order polynomial fit. From the detailed analysis, the result of this fit was found to be similar for the relations between the intensities of peaks at 1606 cm^{-1} to 1640 cm^{-1} (ν_{10}), 1212 to 1224 cm^{-1}, (ν_{13} or ν_{42}), and 1358 to 1372 cm^{-1} (ν_4). It is to be mentioned that the degree of oxygenation (SO_2) can be expressed as $SO_2 = A \times PR + B$, where A and B are the constants characterizing the conditions of the process; the details are mentioned elsewhere.[37] From Fig. 7, it also can be seen that some delay of the oxygenation of deoxygenated RBC is observed at the presence of cND, this delay being more significant for 5 nm cND and deeper deoxygenation.

We have repeated the same experiments several times ($N > 10$) and found the same results. Data presented in Figs. 6 and 7 are from one of the experiments without averaging, since
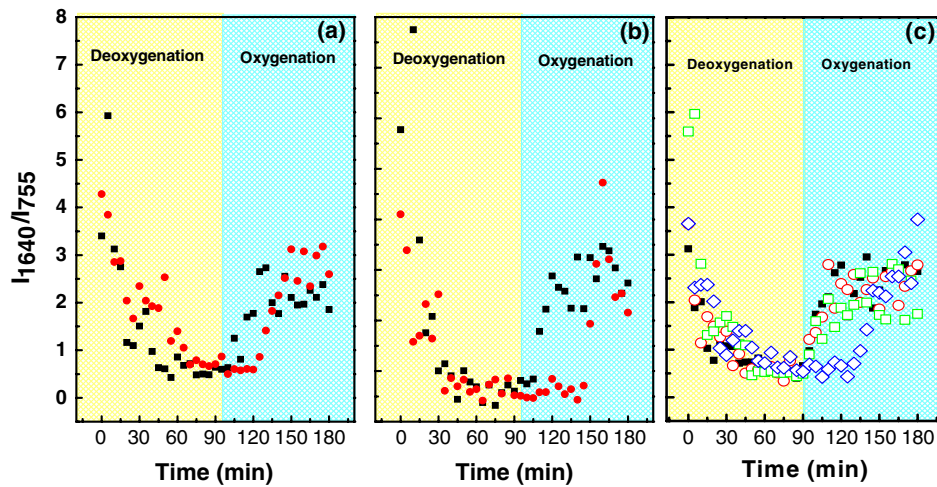
Fig. 6 Oxygenation dynamics of the RBC interacting with ND (A). The time dependence of the deoxygenation followed by oxygenation of (a) RBC (black squares) and RBC interacting with 100 nm cND (red dots); (b) RBC (black squares) and RBC interacting with 5 nm cNd (red dots). The concentrations of cND used was 20 μg/ml. (c) The concentration dependence of the deoxygenation and following oxygenation of (a) RBC (black squares) and RBC interacting with 100 nm cND in different concentrations ($\bigcirc$): 20 μg/ml; ($\square$): 100 μg/ml; ($\diamondsuit$): 1000 μg/ml.
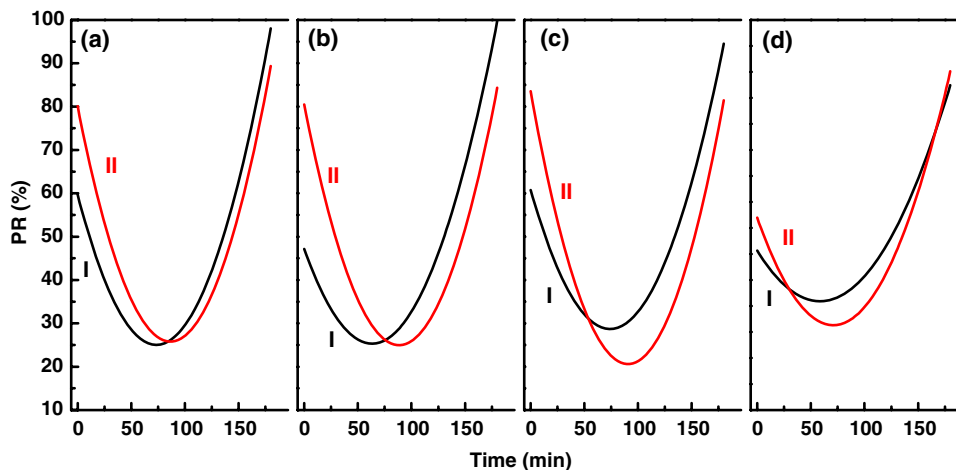

Fig. 7 Oxygenation dynamics of the RBC interacting with ND (B). The peak intensities of the Raman bands for oxygenated (I_{oxy} at 1588 cm^{-1}) and deoxygenated (I_{deoxy} at 1555 cm^{-1}) are compared. The peak ratio (PR) was calculated using [$PR = I_{1588}/(I_{1555} + I_{1588})$], and the dependencies of PR on time during deoxygenation and following re-oxygenation were fitted using standard second order polynomial fit. The results of fitting are shown: (a) I − RBC; II − RBC + 100 nm ND; (b) I − RBC; II − RBC + 5 nm cND; (c) I − RBC; II − RBC + 5 nm ND; (d) I − RBC; II − RBC + 5 nm cND.

the experiments depend on the flow rate of N_2 gas, for example. Details that caused the delay deserve further investigation.

To confirm the oxygenation and deoxygenation of RBC, UV-visible absorption spectra of RBC suspensions, shown in Fig. 8, were measured. The figure depicts the comparison of spectra of the oxygenated and deoxygenated RBCs at the interaction with 100 nm cNDs. In this experiment, RBCs are suspended in PBS solution, the concentration of RBC was 1 μl/ml and concentration of 100 cND suspended in RBC + PBS suspension was 100 μl/ml. Spectra from RBC and RBC with cND revealed similar characteristic peaks. When RBCs are oxygenated, corresponding absorbance peaks appear at 542 and 576 nm; and for deoxygenated RBC, the characteristic absorption is observed at 556 nm. It is to be noted that the absorption of cND is negligible in the visible range. The figure shows that the interaction of cND with RBC does not affect RBC (more precisely, Hb inside the studied RBC) spectra, as well as the Raman spectra shown in Fig. 4.

The RBC membrane structure and state determine the membrane permeability for gases like O_2 and CO_2, and, correspondingly, the ability of RBC for gas transportation. On the other hand, the membrane properties determine the blood rheology. The membrane state and rheological blood properties can be modified by cND interaction with blood. In the microscopic study, the aggregation of the RBC in suspension with cND + RBC has been detected. Note however, that these RBC aggregates have irregular character in contrast to rouleaux aggregation that appears for the RBC in the whole blood. The RBC aggregation is an intrinsic process and characterizes the blood properties as whole, first of all, the blood microcirculation. Usually the aggregation is observed in whole blood, with 2D- or 3D-rouleaux formation. In the aggregation of RBC where the blood plasma constituents are involved, first of all fibrinogen and other large plasma proteins,[39] low density lipoproteins, as well as large polymers like dextran in blood plasma play the major roles.[40,41] According to the bridging model of the
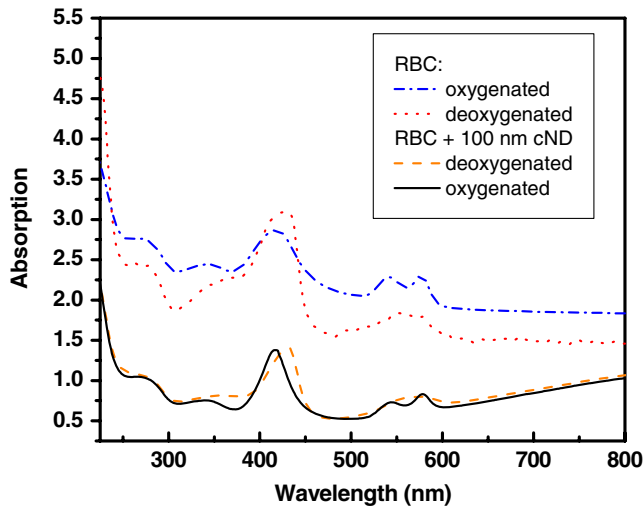
Fig. 8 Absorption Spectra of RBC interacting with cND. UV-visible absorption of RBC + PBS suspension at their oxygenation and deoxygenation *in-situ*, with N_2 purging; comparison with RBC suspension with 100 nm cND. The concentration of RBC is 1 μl/ml and concentration of 100 cND is 100 μl/ml.

Fig. 9 Nanodiamond effect on RBC deformability. Dependences of deformability index of RBC on shear stress: (black square) control RBC suspension; (red dot) RBC with 100 nm cND, concentration 33 μg/ml; (blue triangle) RBC with 100 nm cND, concentration 100 μg/ml. The dotted data are mean values with root mean square deviations after averaging over $n = 8$ blood samples from different individuals. The continuous curves are splines. Measurements were performed within two hours after blood drawing and after 1 h-long incubation of whole blood with cND.

aggregation, the macromolecules participate in the bridges formation; and according to the depletion model, RBC aggregation occurs as a result of a lower localized macromolecules concentration near the cell surface. It leads to osmotic gradient and thus depletion interaction. Electrical and mechanical properties of the membrane also are considered as factors of the aggregation.[42] Thus, changes of the aggregation conditions may be connected with formation of intercellular contacts facilitated by surface aggregated cND, as well as with changes in the membrane properties.[43,44]

The influence of cND on the RBC's mechanical properties is observed via variations of the cell deformability related to its membrane rigidity, which depends on the membrane structure and connects with the membrane functionality.[35,36,45,46] The dependencies of the cell deformability on the shear stress for normal RBC and RBC incubated with 100 nm cND in different concentrations are shown in Fig. 9. It can be seen from the figure that the deformability is decreased when RBCs interact with cND. The decrease in cell deformability (i.e., increasing stiffness or decrease in membrane fluidity) is seen to be more significant for the higher cND concentration. It can be seen that the membrane deformability changes due to the presence of cNDs; thereby the structure of the membrane may change. In the following paragraphs we discuss two issues; first, which structural changes of the membrane can be the reason for the variations in the oxygenation-deoxygenation dynamics, and second, why the effect of cND on oxygenation-deoxygenation cycle of RBCs looks more significant for deoxygenated RBC on the stage of beginning of oxygenation.

The plasma membrane of erythrocytes plays a fundamental role in oxygen transport and in maintaining RBC metabolism.[35] The membrane structural changes created by cND interaction affect the RBC function, and thus can be reasons of the variations in the oxygenation-deoxygenation dynamics. Generally, it has been accepted that the oxygen can penetrate the RBC membrane via direct diffusion. In this case, the membrane permeability for oxygen is limited by the membrane molecules mobility. The mobility was determined by lipids constituting the membrane lipid bilayer with liquid-crystal-like structure, in which
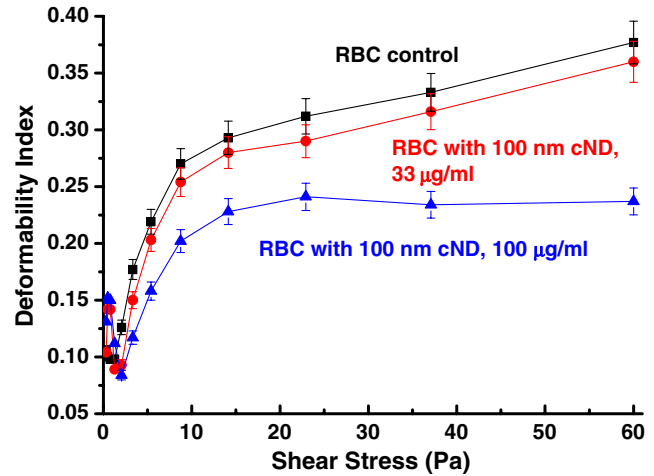
the membrane proteins are incorporated. The cND aggregation on the membrane can decrease the mobility of lipid molecules in the area of contact with cND surface as well as in surrounding areas due to some ordering of liquid-crystal structure of the membrane. One could assume that it decreases the oxygen transmembrane transport and correspondingly the rate of oxygenation and deoxygenation in RBC, although some doubts exist concerning the role of direct diffusion permeability of the RBC membrane for oxygen.[36,46] The role of channels and pores in the oxygen permeability is discussed, e.g., it was suggested that RBC membrane can modulate the function of hemoglobin, but the details are still not clear and incomplete.[47]

The interaction of proteins with ND may alter their structure and activity.[33,48,49] Presumably, if ND interacts extensively with the membrane proteins, it can modify the structure and functionality, including transport proteins involved in oxygen transport. As a result, interaction of ND with the membrane alters oxygen and other important substances concentrations in the RBC cytoplasm. Additionally, it has been already shown that the organic phosphate, i.e., 2,3-diphosphoglycerate (2, 3 DPG) in the RBC, binds with Hb (with β-sheets) and affects the Hb affinity to oxygen (oxygen binding capacity), facilitating the detaching O_2 from Hb molecule.[35] It is important that 2, 3 DPG is involved in the interaction of Hb with membrane, particularly with the band three protein. Thus, varying membrane state can vary conditions of 2, 3 DPG interaction with the membrane; and correspondingly, the interaction between Hb and 2, 3 DPG changes. So, the predominant affinity of 2, 3 DPG to deoxy-Hb relatively oxy-Hb may be one of the reasons why the observed effect of cND on the oxygenation-deoxygenation cycle differs for different oxygenation states.

Connection between the oxygenation-deoxygenation of RBC and the RBC mechanical properties has been discussed[50] with consideration of RBC cell membrane fluctuations (CMF). They were observed involving local cell membrane displacements and bending deformability of the cell membrane. RBC

deoxygenation results in a decrease of the CMF; when deoxygenated cells (revealing a small amplitude of displacement) are re-oxygenated, their amplitude of fluctuation is restored. The CMF are shown strongly metabolically dependent, and they are correlated with oxygenation-deoxygenation cyclic changes in metabolite concentrations. It is shown that hemoporphirine conformation (strongly connected with Hb's ability to bind and release the ligands) is affected by Hb binding to the inner surface of erythrocyte membrane and membrane fluidity.[36] One can suppose that when the nanoparticle adsorption on the membrane increases the membrane rigidity, probably, the membrane transformation into a state with higher CMF can be obstructed. In turn, it may delay the beginning of re-oxygenation. Thus, probable mechanisms, involved in the interaction of ND with RBC and determining the ND influence on RBC are proposed. However, complete understanding needs further investigations in the same direction.

4 Conclusion

In conclusion, interaction of 5 and 100 nm cNDs with RBCs has been studied. We show that the 100 nm cNDs are localized around RBCs, whereas 5 nm cND penetrate inside the RBCs. The 5 and 100 nm sized cND with 5 and 50 μg/ml concentrations are nontoxic for RBCs. The hemolytic effect of cND does not exceed 2 to 4% with respect to 0.5% TritonX 100, which for Triton was normalized to 100%. Raman spectra for both sized cND do not show any transformations for the RBCs, thereby signifying no structural transformations in Hb. It is observed that the 5 and 100 nm cND does not affect significantly the deoxygenation dynamics. However some delay of the oxygenation is observed for the RBC deoxygenated in the presence of 100 nm cND and is concentration dependent. On the other hand, RBC with 5 nm sized cND show deeper deoxygenation followed by observably more delay of the oxygenation for deoxygenated RBC. Similar to Raman results, UV-visible absorption spectra confirmed that the interaction of cND with RBC does not affect Hb oxygenation state inside the studied RBC. Deformability analysis showed that deformability of RBCs decreases significantly for higher concentration of 100 nm cND. Finally, it is shown that 100 nm cND interact with the RBCs and can be used to study and manipulate the RBC's membrane properties.

References

1. J.-I Chao et al., "Nanometer-sized diamond particle as a probe for biolabeling," *Biophys. J.* **93**, 2199–2208 (2007).
2. E. Perevedentseva et al., "The interaction of the protein lysozyme with bacteria *E. coli* observed using nanodiamond labeling," *Nanotechnology* **18**, 315102 (2007).
3. Y.-R. Chang et al., "Mass production and dynamic imaging of fluorescent nanodiamonds," *Nat. Nanotechnol.* **3**, 284–288 (2008).
4. A. M. Schrand, H. S. A. Ciftan, and O. A. Shenderova, "Nanodiamond particles: properties and perspectives for bioapplication," *Crit. Rev. Solid State Mater. Sci.* **34**, 18–74 (2009).
5. P.-H. Chung et al., "Spectroscopic study of bio-functionalized nanodiamonds," *Diam. Relat. Mater.* **15**, 622–625 (2006).
6. M. Chen et al., "Nanodiamond-mediated delivery of water-insoluble therapeutics," *ASC Nano* **3**, 2016–2022 (2009).
7. K. Ramser et al., "A microfluidic system enabling Raman measurements of the oxygenation cycle in single optically trapped red blood cells," *Lab. Chip* **5**, 431–436 (2005).
8. B. R. Wood and D. McNaughton, "Micro-Raman characterization of high- and low-spin heme moieties within single living erythrocytes," *Biopolymers* **67**, 259–262 (2002).
9. B. R. Wood, L. Hammer, and D. McNaughton, "Resonance Raman spectroscopy provides evidence of heme ordering within the functional erythrocyte," *Vib. Spectrosc.* **38**, 71–78 (2005).
10. K. Ramser et al., "Importance of substrate and photo-induced effects in Raman spectroscopy of single functional erythrocytes," *J. Biomed. Opt.* **8**, 173–178 (2003).
11. S. Rao et al., "Raman study of mechanically induced oxygenation state transition of red blood cells using optical tweezers," *Biophys. J.* **96**, 209–216 (2009).
12. A. P. Puzyr et al., "Destruction of human blood cells in interaction with detonation nanodiamonds in experiments in vitro," *Diam. Relat. Mater.* **13**, 2020–2023 (2004).
13. Y. Yuan et al., "Biodistribution and fate of nanodiamonds *in vivo*," *Diam. Relat. Mater.* **18**, 95–100 (2009).
14. B. M. Rothen-Rutishauser et al., "Interaction of fine particles and nanoparticles with red blood cells visualized with advanced microscopic techniques," *Environ. Sci. Technol.* **40**, 4353–4359 (2006).
15. V. Wiwanitkit, A. Sereemaspun, and R. Rojanathanes, "Visualization of gold nanoparticle on the microscopic picture of red blood cell: implication for possible risk of nanoparticle exposure," *Stoch. Env. Res. Risk A* **22**, 583–585 (2008).
16. I. I. Slowing et al., "Mesoporous silica nanoparticles for reducing hemolytic activity towards mammalian red blood cells," *Small* **5**, 57–62 (2009).
17. M. A. Dobrovolskaia et al., "Interaction of colloidal gold nanoparticles with human blood: effects on particle size and analysis of plasma protein binding profiles," *Nanomed. Nanotechnol. Biol. Med.* **5**, 106–117 (2009).
18. F.-Y. Cheng et al., "Characterization of aqueous dispersions of Fe_3O_4 nanoparticles and their biomedical applications," *Biomaterials* **26**, 729–738 (2005).
19. S. Q. Li et al., "Nanotoxicity of TiO_2 nanoparticles to erythrocyte in vitro," *Food Chem. Toxicol.* **46**, 3626–3631 (2008).
20. E. Chambers and S. Mitragotri, "Long circulating nanoparticles via adhesion on red blood cells: mechanism and extended circulation," *Exp. Biol. Med.* **232**, 958–966 (2007).
21. E. Chambers and S. Mitragotri, "Prolonged circulation of large polymeric nanoparticles by non-covalent adsorption on erythrocytes," *J. Control. Release* **100**, 111–119 (2004).
22. J.-S. Tu et al., "Size-dependent surface CO stretching frequency investigations on nanodiamond particles," *J. Chem. Phys.* **125**, 174713 (2006).
23. P.-H. Chung, E. Perevedentseva, and C.-L. Cheng, "The particle size-dependent photoluminescence of nanodiamonds," *Surf. Sci.* **601**, 3866–3870 (2007).
24. S. Yu. Nikitin, A. V. Priezzhev, and A. E. Lugovtsov, "Laser diffraction by the erythrocytes and deformability measurements," in *Advanced Optical Flow Cytometry*. V. V. Tuchin, ed., Wiley-VCH Verlag GmbH, Weinheim, Germany, 133–154 (2011).
25. S. Yu. Nikitin, A. E. Lugovtsov, and A. V. Priezzhev, "On the problem of the diffraction pattern visibility in laser diffractometry of red blood cells," *Quant. Electron.* **40**, 1074–1076 (2011).
26. M. Uyuklu, H. J. Meiselman, and O. K. Baskurt, "Effect of hemoglobin oxygenation level on red blood cell deformability and aggregation parameters," *Clin. Hemorheol. Micro.* **41**, 179–188 (2009).
27. M. V. Berridge, P. M. Herst, and A. S. Tan, "Tetrazolium dyes as tools in cell biology: new insights into their cellular reduction," *Biotechnol. Annu. Rev.* **11**, 127–152 (2005).
28. E. Kennett, "Transmembrane electron transport systems in erythrocyte plasma membranes," University of Sydney, School of Molecular and Microbial Biosciences, Sydney, Australia, pp. 135–162 (2006).

29. C. A. Best et al., "Red blood cell fatty acid ethyl esters: a significant component of fatty acid ethyl esters in the blood," *J. Lipid Res.* **44**, 612–620 (2003).
30. L. N. Yuldasheva et al., "Colesterol-dependent hemolitic activity of *Passiflora quadrangularis* leaves," *Braz. J. Med. Biol. Res.* **38**, 1061–1070 (2005).
31. M. A. Dobrovolskaia et al., "Method for analysis of nanoparticle hemolytic properties in vitro," *Nano Lett.* **8**, 2180–2187 (2008).
32. C. M. Goodman et al., "Toxicity of gold nanoparticles functionalized with cationic and anionic side chains," *Bioconjug. Chem.* **15**, 897–900 (2004).
33. E. V. Perevedentseva et al., "Laser-optical investigation of nanodiamond particles effect on the structure and functional properties of proteins," *Quant. Electron.* **40**, 1089–1093 (2011).
34. H. D. Wang et al., "Study on protein conformation and adsorption behaviors in nanodiamond particle-protein complex," *Nanotechnology* **22**, 145703 (2011).
35. M. C. De Rosa et al., "The plasma membrane of erythrocytes plays a fundamental role in the transport of oxygen, carbon dioxide and nitric oxide and in the maintenance of the reduced state of the heme iron," *Gene* **398**, 162–171 (2007).
36. D. Dumas et al., "Membrane fluidity and oxygen diffusion in cholesterol-enriched erythrocyte membrane," *Arch. Biochem. Biophys.* **341**, 34–39 (1997).
37. I. P. Torres Filho et al., "Measurement of hemoglobin oxygen saturation using Raman microspectroscopy and 532-nm excitation," *J. Appl. Physiol.* **104**, 1809–1817 (2008).
38. B. R. Wood and D. McNaughton, "Raman excitation wavelength investigation of single red blood cells *in vivo*," *J. Raman Spectrosc.* **33**, 517–523 (2002).
39. A. V. Priezzhev, N. N. Firsov, and J. Lademann, "Light scattering diagnostics of red blood cell aggregation in whole blood samples," in *Handbook of Optical Biomedical Diagnostics*, V. V. Tuchin, ed., SPIE Press, Bellingham, USA, pp. 651–674 (2002).
40. B. Neu, R. Wenby, and H. J. Meiselman, "Effects of dextran molecular weight on red blood cell aggregation," *Biophys. J.* **95**, 3059–3065 (2008).
41. V. Schechner et al., "Plasma dependent reduction in red blood cell aggregation after dextran sulfate low-density lipoprotein apheresis-implications for rheological studies," *Ther. Apher. Dial.* **9**, 379–384 (2005).
42. S. Jovtchev et al., "Role of electrical and mechanical properties of red blood cells for their aggregation," *Colloids Surf. A* **164**, 95–104 (2000).
43. S. Svetina and P. Ziherl, "Morphology of small aggregates of red blood cells," *Bioelectrochemistry* **73**, 84–91 (2008).
44. G. Barshtein, D. Wajnblum, and S. Yedgar, "Kinetics of linear rouleaux formation studied by visual monitoring of red cell dynamic organization," *Biophys. J.* **78**, 2470–2474 (2000).
45. N. Mohandas and P. G. Gallagher, "Red cell membrane: past, present, and future," *Blood* **112**, 3939–3948 (2008).
46. H. Buchwald et al., "Plasma cholesterol: an influencing factor of red blood cell oxygen release and cellular oxygen availability," *J. Am. Coll. Surg.* **191**, 490–497 (2000).
47. I. I. Ivanov et al., "Oxygen channels of erythrocyte membrane," *Dokl. Biochem. Biophys.* **414**, 137–140 (2007).
48. E. Perevedentseva et al., "Characterizing protein activities on the lysozyme and nanodiamond complex prepared for bio applications," *Langmuir* **27**, 1085–1091 (2011).
49. Z. Wu, B. Zhang, and B. Yan, "Regulation of enzyme activity through interactions with nanoparticle," *Int. J. Mol. Sci.* **10**, 4198–4209 (2009).
50. S. Tuvia, S. Levin, and R. Korenstein, "Oxygenation-deoxygenation cycle of erythrocytes modulates submicron cell membrane fluctuations," *Biophys. J.* **63**, 599–602 (1992).